Temperature profiles from airborne pyrgeometer measurements of broadband terrestrial radiation.

K. Wolf, A. Ehrlich, M. Wendisch

Institute of Meteorology, Stephanstr. 3, 04103 Leipzig, E-Mail: kevin.wolf@uni-leipzig.de

Summary

Profiles of broadband terrestrial radiation from airborne pyrgeometer measurements aboard research aircraft Polar 5 obtained during the VERDI campaign in 2012 were used to derive vertical temperature profiles. The retrievals were performed utilizing radiative transfer simulations by libRadtran (Mayer and Kylling, 2005). Manually changing the temperature of the input file for the simulations resulting calculated profiles of terrestrial irradiance were compared with measured profiles and iterated until best agreement.
The selected test case shows the possibility of this technique and reveals several possible improvements. The algorithm has to be optimized to adapt the modelling temperature profile automatically using least-square error minimization between measured and modelled irradiance profiles. Additionally the vertical resolution has to be increased to consider small-scale variations. Using humidity and pressure profiles from ground-based observations and nearby radiosoundings significantly improves the retrieved temperature profiles.

Zusammenfassung

Vertikalprofile der breitbandigen terrestrischen Strahlung von flugzeuggetragenen Pyrgeometermessungen an Bord des Forschungsflugzeuges Polar 5 während der VERDI Kampagne in 2012 wurden genutzt, um Vertikalprofile der Temperatur abzuleiten. Das Retrieval erfolgte mit Hilfe von Strahlungstransfersimulationen unter der Verwendungung von libRadtran (Mayer and Kylling, 2005). Dazu wurde die Temperatur der Modellatmosphäre variert, bis eine bestmögliche Übereinstimmung von gemessenem und modellierten Irradianzprofil erzielt wurde.
Der ausgesuchte Testfall zeigt das Potential dieser Technik und mögliche Verbessungsansätze. So muss der verwendete Algorithmus automatisiert werden, indem das modellierte Strahlungsprofil mit Hilfe eines Iterationsverfahrens und der Methode der kleinsten Fehlerquadrate an das gemessene Profil angepasst wird. Zusätzlich ist eine Erhöhung der vertikalen Auflösung von 50 m auf 10 m Schritte nötig, um kleinskalige Fluktuationen zu berücksichtigen. Die Verwendung von bodengebundenen Beobachtungen und nahegelegenen Radiosondenaufstiegen in der Modellatmosphäre führt zu einer weiteren signifikanten Verbesserung der abgeleiteten Temperaturprofile.

1 Introduction

The vertical temperature profile of the atmosphere is of importance for processes like convection and turbulence. During summertime in the midlatitudes the temperature profile determines the development of strong vertical motions and corresponding thunderstorms which can cause massive destruction to buildings and infrastructure. Storm development mostly results from unstable atmospheric conditions which are present when the temperature decreases with more then $\Gamma_d = 0.98\,\mathrm{K}\,100\mathrm{m}^{-1}$ which is the dry-adiabatic temperature gradient. A lifted air-parcel will be warmer than the surrounding air resulting in a density gradient which implies an additional force accelerating the air-parcel upwards. In an unstable atmosphere small-scale vertical deflections from the initial position result in self-intensifying upward motions increasing the chance of severe weather development. In case of neutral layering the temperature of the atmosphere decreases with the dry-adiabatic temperature gradient. The temperature of the air-parcel and the surrounding air is similar and no external force accelerates the air-parcel. Air-parcels in such atmospheric conditions will remain at a constant hight. If the atmosphere is stable the temperature of the air is decreasing faster then Γ_d. Every air-parcel which is forced out of the inertial position will return to the same hight level.
Despite the mentioned influence on convection the vertical temperature profile is of mayor importance for thermodynamic processes and the radiative budget of the Earth. The temperature of each atmospheric layer mainly determines the intensity of emitted terrestrial radiation. In Arctic regions terrestrial radiation dominates the radiation budget because the solar part is less resulting from low solar incident radiation due to low Sun elevations. Investigation of temperature profiles under different atmospheric conditions is important to establish long-term trends of the Arctic climate and global climate modelling. In resent times there are a lot of efforts trying to explain Arctic Amplification which can be caused by Laps-rate and Planck feedback mechanisms where the temperature profile is the driving factor (Pithan and Mauritsen, 2014). The method of deriving vertical temperature profiles from irradiation measurements can also be inverted to determine the change of the radiation budget of the Earth's atmosphere in Arctic regions due to climate change and changing temperature profiles.
Up to now several methods exist to derive vertical temperature profiles. One of them are radiosoundings which provide a low-cost and easy way to measure. Such measurements are performed all over the world in a continuous way but are restricted to land. An other possibility are active and passive remote sensing instruments like microwave profilers which can derive vertical profiles of temperature and humidity. These instruments have to be operated with assumptions and parametrizations which can cause large errors (Pospichal, 2011). Microwave profilers can be operated as ground-base instruments or on satellites like the Aqua satellite which is part of the A-Train-constellation opperated by the National Aeronautics and Space Administration (NASA). Utilizing several infrared channels this satellite is able to derive a daily average of the vertical temperature profile with an accuracy of 1 K for an atmospheric layer with a thickness of about 1 000 m (Kempler, 2013). This vertical resolution is not sufficient for climate modelling. All mentioned techniques have the disadvantage that they are restricted to continents or have low spatial resolution. In contrast, airborne measurements can be a suitable tool allowing large-scale measurements in regions which can not be probed in any other way. Furthermore many regions of the Arctic are hard to reach and only accessible by air-

craft. Up to now measurements over oceans and in the polar regions which cover nearly 70 % of the Earth are rare resulting in a lack of data for climate modelling. To increase global data set results of the water and ice covered regions airborne measurements are necessary. They can provide in-situ measurements from regions of interest which are not accessible by other methods like observations from the ground. Improving airborne remote sensing techniques opens a new opportunity to derive vertical temperature profiles in remote areas.

2 Radiation properties

Every body with a temperature above 0 K emits radiation with a specific intensity and a maximum at a specific wavelength which depends on the bodies temperature. Both can be calculated by Plancks law and Wiens displacement law. The emitted radiance in dependence of temperature and wavelength is calculated by:

$$I_\lambda(T) = \frac{2hc^2}{\lambda^5} \frac{1}{e^{\frac{hc}{\lambda k_B T}} - 1} \tag{2.1}$$

$I_\lambda(T)$ is the spectral radiance, h the Planck constant, k_B the Boltzmann constant, c the speed of light, λ the selected wavelength and T the temperature. The radiance is given in units of $\mathrm{W\,m^{-2}\,nm^{-1}\,sr^{-1}}$. This equation is valid for black bodies in thermodynamic equilibrium only. Calculating the first derivation of the Plancks law one get Wiens displacement which gives the wavelength position of the maximum emitted radiance. With a surface temperature of about 6 000 K the maximum of emitted radiation of the Sun is in the range of the shortwave electromagnetic spectrum. Contrarily the Earth emits radiation mainly in the terrestrial spectrum because of an average surface temperature between 250 K and 300 K. One distinguish between shortwave, solar radiation and longwave, terrestrial radiation at a wavelength of 4 μm. This threshold was selected because 99 % of the solar radiation from the Sun is emitted below 4 μm. Above this value the radiation is called longwave, terrestrial radiation (Petty, 2006).
The Stefan-Boltzmann law is obtained by integrating the Planck law over all wavelength and all solid angles resulting in:

$$F = \varepsilon \sigma T^4 \tag{2.2}$$

F is called irradiance, ε is the emissivity parameter, σ is the Stefan-Boltzmann-constant and T is the temperature of the black body. The irradiance is given in $\mathrm{Wm^{-2}}$. The Stefan-Boltzmann-law is important for calculation of the broadband, terrestrial radiation transport. Rearranging the equation the brightness temperature T_b can be calculated by:

$$T_b = \sqrt[4]{\frac{F}{\varepsilon \sigma}} \tag{2.3}$$

T_b is the temperature an idealized black body in thermal equilibrium would have when emitting the same amount of radiation a grey body does at a specific frequency. The brightness temperature is frequently used in investigations of the terrestrial radiation budget of the Earth. The black body is a simplification in radiation transfer theory. It is defined as an object which emits and absorbs radiation completely. Therefore emission coefficient and absorption coefficient are equal to one. With this assumption the irradiance can directly transformed into the corresponding brightness temperature and vice versa. Objects with emission and absorption coefficients lower then one are called grey bodies.
Another assumption about emission of terrestrial radiation is isotropy meaning that radiation is emitted in all directions evenly. Therefore the azimuthal dependence of emitted radiation is negligible and attitude corrections of optical inlets can be neglected.

2.1 Absoprtion and emission by gas molecules

For simplification the Earth atmosphere can be regarded as a black body. Therefore, Wiens displacement-law and the Stefan-Boltzmann-law can be utilized. Measurements of broadband, terrestrial radiation are possible due to absorption and emission by gas molecules. In the following section mechanisms will be explained which cause absorption and emission.
Atoms and molecules are able to store energy. This can be done in discrete, quantized amounts only which causes specific emission and absorption lines in the spectra of gases. Due to the Kirchhoff-law absorption lines are equal to emission lines. When atoms or molecules receive energy from photons (absorption) the electrons of the atoms change to an exciting state with higher energy level then in the inertial position. This results in an unstable situation and the electron returns to its initial state within milliseconds emitting the same amount of energy. If the incident energy is to high or to low for electron state transitions, then the electron remains at the current electron level and no absorption occurs. Because only discrete amounts of energy can be absorbed and emitted each atom and molecule has its own signature of absorption and emission lines in the electromagnetic spectrum. Due to overlapping and broadening of these lines absorption and emission bands develop.
Absorption and emission lines in the UV spectrum are caused by electron transitions because of the high amounts of energy needed to change the state of an electron. Gases which are important for UV absorption are oxygen and ozone which absorb nearly all incoming UV radiation. Oxygen mainly absorbs in the wavelength range between 100 nm and 242 nm as well as 690 nm and 760 nm. Ozone shows an absorption band between 200 nm and 850 nm (Wendisch and Yang, 2012).
In contrast to atoms absorption by molecules is much more complex due to the combination of different types of atoms and possible covalent bondings between atoms. Additionally molecules can transform absorbed energy into translation movements, vibration (periodic change of bonding distance) and rotation around itself. This enhances the number of possible absorption and emission lines and creates spectral bands.
The amount of energy stored in vibration, translation movements and rotation of the molecules is much less compared to electron transitions and appears at longer wavelength in the visible and infrared range of the electromagnetic spectrum.

For atmospheric radiation processes three gases are of major importance. These are water vapour, carbon dioxide and ozone. Water vapour is nearly 100 % transparent for the UV, the visible and far infrared wavelength region. Most of the absorption takes place in the near infrared. Water vapour absorbs about 70 % of the total amount of absorbed incoming solar radiation. Terrestrial radiation emitted from the Earth is absorbed by water vapour in the range of 60 %. This indicates the importance of water vapour for radiation in the near infrared wavelength region. Carbon dioxide and ozone are two gases which cause some absorption and emission in the near infrared.
Absorption and emission is present all the time and is a continuous process. Because of the density of the air the free path length for infrared radiation is in the range of several meters up to 100 meters (Geiger et al., 1995). Therefore pyrgeometer receive radiation from the nearest air layers only and measurements of vertical brightness temperature profiles of such layers are possible.

3 Measurement

Utilized measurements were taken during the VERDI campaign in the year 2012. Research flights started at Inuvik, Canada and were performed using the Polar 5 (P5) research aircraft of the Alfred Wegener Institute (AWI). For this case study one flight from the 22nd of April between 17:55 UTC and 23:20 UTC was selected. To derive vertical temperature profiles an appropriate flight pattern has to be chosen. This was present between 21:12 UTC and 21:26 UTC when the aircraft changed flight altitude performing a constant ascent rate. During this time period the aircraft flew over the Beaufort Sea northern the Northwest Territories.
For this case datasets of two pyrgeometers are analyzed. The pyrgeometers are CGR4 made by Kipp & Zonen. Details about installation, performance and operation of these instruments can be found at (Kipp & Zonen, 2006). Both were mounted at the outside of the aircraft lower and upper fuselage for measuring upward and downward terrestrial radiation. Additionally the temperature, humidity and pressure was recorded by the onboard meteorological instrumentation. Utilizing Global Positioning System (GPS) the position and hight of the aircraft was determined.

3.1 Pyrgeometer

Pyrgeometers are used to measure infrared radiation in the wavelength region between 4.5 μm and up to 100 μm. The housing is made out of aluminium to provide good temperature and mechanical stability for ground and airborne measurements. The spectral coverage of the Kipp & Zonen CGR4 ranges between 4.5 μm and 42 μm. The CGR4 has a flat dome which allows a field of view of 180° and a good cosine characteristic of the sensor inlet. A flat dome can be coated much more even and reduces measurement uncertainties. The coating acts as an interference filter which transmits radiation in the wavelength region of interest and cuts off radiation below 4.5 μm. The dome is made out of silicon which allows transmittance up to 42 μm. Because every sensor shows different response the instrument has to be calibrated to a reference instrument situated at the World Radiation Center in Davos, Switzerland.
The irradiance is calculated by the following equation:

$$F_d = \frac{U}{S} + 5.67 \cdot 10^{-8} \cdot T^4 \tag{3.1}$$

with U the output voltage of the pyrgeometer, T the temperature of the housing and F_d the measured irradiance by the reference pyrgeometer. To determine the calibration constant S the equation is transformed to:

$$S = \frac{U}{F_d - 5.67 \cdot 10^{-8} \cdot T^4} \tag{3.2}$$

Measurement errors result from the temperature dependence of the sensor, the response time and the intensity of the incoming radiation because of non-linearity of sensor sensitivity. The sensitivity of the sensor depends on the absolute temperature. Therefore all calibrations are performed at 20 °C. For the CGR4 the temperature sensitivity is reduced by an integrated circuit which additionally compensated temperature changes of the housing. External corrections do not have to be applied. The deviation from temperature linearity for the CGR4 is reported to be lower than 1 % between −20 °C and 50 °C and below 5 % between −40 °C and −20 °C (Kipp & Zonen, 2006).
Non-linearity of the sensor means that high / low irradiances may be underestimated or vice versa. To characterize the deviation from linearity the pyrgeometer is illuminated with a standardized lamp with 250 $\mathrm{W\,m^{-2}}$. Then the measurement is subtracted from the theoretic value of the standardized lamp and normalized to 100 $\mathrm{W\,m^{-2}}$ getting the deviation from linearity. For the CGR4 the deviation is reported to be lower than 1 % (Kipp & Zonen, 2006).
The response time τ is the duration the instrument needs to react to sudden changes of environmental conditions because of sensor inertia. It is defined as the time until the difference of the signal is below $1\,e^{-1}$ ($\approx 33\,\%$) of the absolute signal. Kipp & Zonen, 2006 reports τ to be under 6 s. Because of the good temperature stability, constant sensor sensitivity and high temporal resolution the CGR4 is feasible to be operated on aircraft for measuring vertical profiles.

3.1.1 Meteorological Parameters

For deriving vertical temperature profiles radiative transfer models are used. These need vertical profiles of humidity and pressure. Therefore, measurements of the aircraft are applied in the models. Additional measurements of dropsondes and radiosonds from Inuvik, Canada are available. Vertical temperature profiles measured by the aircraft are used to validate the modelled vertical temperature profile. Dropsonde measurements were performed with the VAISALA AVAPS Dropsonde-System (Vaisala, 2010).

Temperature

The temperature measurement was performed with a total temperature probe manufactured by Goodrich. The sensor includes a Pt-100 resistance wire mounted inside a special designed housing to avoid condensation, impact of ice on the sensor wire and to

reduce the influence of radiation on the measurement. The P5 aircraft is equipped with the Model 102 configuration B which supports deicing making it possible to be utilized in Arctic and subarctic regions. The time constant is specified under 1 s and measurement uncertainties are reported to be within $\pm 0.25\,^{\circ}\mathrm{C}$ (Stickney et al., 1994). Together with a climbing rate of 2.88 $\mathrm{m\,s^{-1}}$ of the aircraft the resolution of the vertical temperature profile is about 2.8 m.
Airborne temperature measurements are effected by two components. One are dynamic effects caused by the airflow around the sensor. Air hitting the sensor housing is stopped immediately to zero velocity and kinetic energy is transformed into thermal energy heating up the sensor. This results in systematically overestimation of the temperature. This biased temperature is called Total Air Temperature (TAT). It is assumed that all kinetic energy is transformed into thermal energy. With regard to the relative velocity difference between the horizontal wind vector and the aircraft and the density of the air the so called Static Air Temperature (SAT) is calculated. This is the temperature of the undisturbed air. With increasing aircraft velocity and flight level the difference between TAT and SAT increases and corrections have to be applied. Under simplified conditions equation 3.3 can be used to determine the SAT.

$$SAT = \frac{TAT}{(\frac{\kappa - 1}{2})M^2 + 1} \tag{3.3}$$

In this equation the aircraft velocity M in the unit Mach is considered only. For transforming kinetic energy into thermal energy the adiabatic exponent κ is needed.
The second factor which influences temperature measurements is the deicing of the sensor. Inside clouds with supercooled droplets this function is activated to avoid internal icing. This causes a temperature offset of $0.5\,^{\circ}\mathrm{C}$. Temperature measurements during an activated de-icing have to be corrected for this offset. Fig. 1 shows vertical temperature profiles measured by the aircraft P5 (solid line), the dropsonde (dotted line) and the radiosounding (dashed line). The grey area shows the uncertainty range of the aircraft measurement. Additionally the temperature profile of the modelling atmosphere (afglsw) for subarctic winter regions provided by Anderson et al. (1986) of the radiative transfer model is included by the dash-dotted line. The plot shows, that the temperature of the modelling atmosphere is systematically lower than the measured profile by P5 and the dropsonde. In contrast the temperature of the radiosonde is much larger than the P5 measurement. This is mainly cause by spatial difference of 500 km between the measurement area and Inuvik where the radiosonde was launched. Furthermore a temporal difference of 2.5 h has to be considered. Best agreement is visible between the measurement of the P5 sensor and the dropsonde. Beginning at 300 m and reaching up to 1 000 m a strong inversion is present. The strongest gradient appears between 300 m and 500 m. Above 1 000 m the temperature decreases constantly.

Water Vapour

Water vapour is the mayor constituent in the atmosphere which causes absorption and emission of terrestrial radiation. Therefore measurements of humidity taken onboard

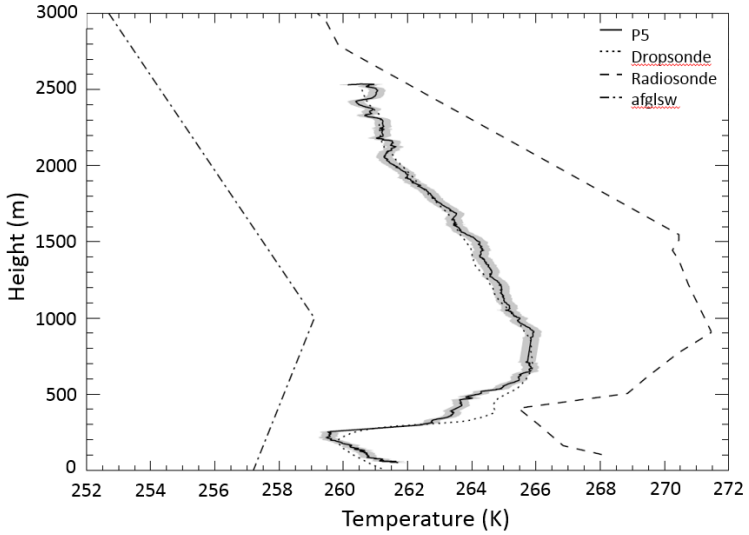

Figure 1: *Measured vertical temperature profile by P5 aircraft (solid line), dropsonde (dotted line) and radiosonde (dash dashed). Uncertainty range of P5 sensor is marked by the grey area. Temperature profile of afglsw standard atmosphere is given by dash-dotted line.*

the P5 aircraft were used in the radiative transfer model. The data were obtained by a CR-2 of Buck Research Instruments which is developed for airborne applications. It bases on a dew-point mirror which is cooled until condensation begins. This results in a decreased reflection of the mirror and can be registered by photo-diode sensors. Using the temperature and density of the surrounding air the absolute and relative humidity is calculated. The instrument can be operated between $-80\,^{\circ}\mathrm{C}$ and $40\,^{\circ}\mathrm{C}$ with an accuracy of $\pm 0.1\,^{\circ}\mathrm{C}$ corresponding to an accuracy of $\pm 1\,\%$ in relative humidity. The time constant is specified to be lower than 1 s (Buck Research Instruments, 2009) resulting in a vertical resolution of the profile of 2.8 m considering the accent rate of the aircraft. The obtained vertical humidity profile is shown in Fig. 2. Below 400 m the radiosonde registered lower values of humidity compared to the CR-2 and the dropsonde. Above this hight the radiosonde measured systematically higher relative humidities compared to the other instruments. Beginning at 1 500 m the difference increases significantly. Below, the vertical profile of radiosonde and dropsonde have similar patterns and differences can be explained by the spatial and temporal difference between the measurement. Furthermore humidity is strongly variable and can change significantly within short distances. It is possible that the radiosonde was launched inside a completely different airmass.

Humidity measured by CR-2 and dropsonde agree in most hight levels showing a similar pattern. Differences of 10 % relative humidity are reported few meters above surface. The decrease of humidity at 300 m hight is not registered by the CR-2 as the dropsonde does. An even larger difference appears between 600 m and 1 600 m when the dropsonde measures up to 15 % less than the CR-2. A reasonable explanation could be a cloud or very humid layer which was probed by the CR-2 aboard the aircraft but not by the dropsonde.

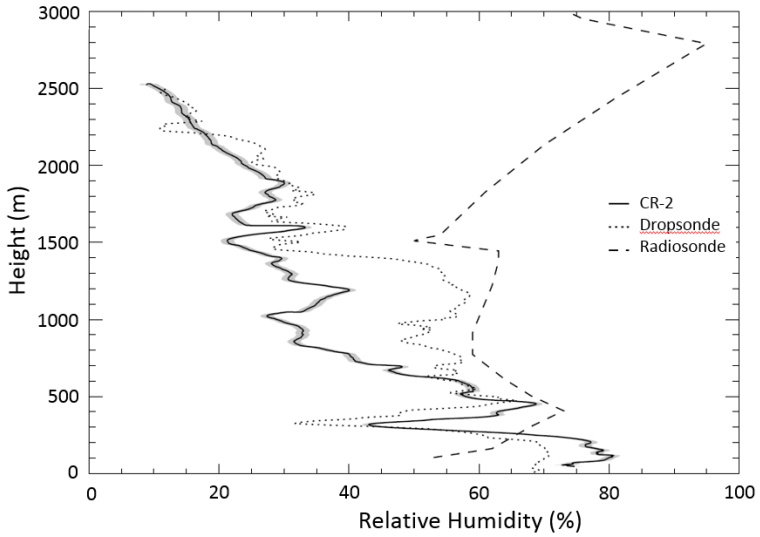

Figure 2: *Measured vertical humidity profile by CR-2 onboard the aircraft (solid line), dropsonde (dotted line) and radiosonde (dash dashed). Uncertainty range of CR-2 sensor is marked by the grey area.*

Pressure

Air pressure was measured by basic meteorology of the research aircraft and recorded together with all flight parameters by the Air Data Computer. Analysing this data a systematic positive offset was detected. Therefore the dropsonde measurements are implemented in the radiative transfer simulations. Fig. 3 shows vertical pressure profiles measured by the dropsonde and radiosonde. Additionally the profile of the afglsw standard atmosphere is included. In contrast to temperature and humidity the pressure profiles agree well and only slight deviations are visible.
Depending on atmospheric pressure the amount of molecules in an imaginary air parcel changes. Higher pressure increases the number of particles per air parcel which can interact with radiation resulting in increased absorption and emission. Therefore the air pressure must be regarded in models for temperature profile retrieval.

4 Retrieval of Vertical Temperature-Profile

In the following section all measured and simulated irradiances are converted into brightness temperatures by applying the Stefan-Boltzmann-law. The simulation were performed with libRadtran (Mayer and Kylling, 2005). With these libraries and programs it is possible to simulate solar and terrestrial radiation in the Earth atmosphere and interactions with aerosols and gas molecules.
First simulations were performed with the standard profile for humidity and pressure for subarctic regions during winter (afglsw) which is adequate to the location of Inuvik and the time of year the measurements were performed (model A). Later these standard parameters were substituted by the humidity measurements of the CR-2 (model B) and the pressure measurement of the dropsonde (model C) to ensure simulations which represent the actual situation during the flight. Using measured profiles instead of standardized profiles better retrieval results are assumed especially for high variable parameters

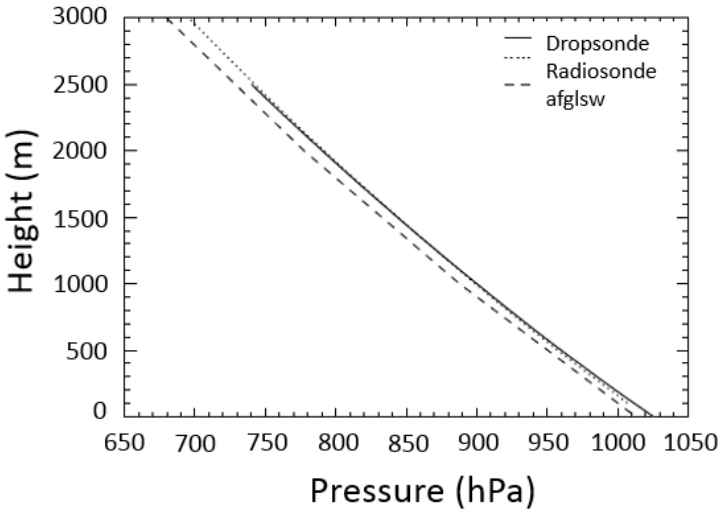

Figure 3: *Measured vertical pressure profile by dropsonde (solid line) and radiosonde (dotted line). Additionally the pressure profile of the standard atmosphere (dashed line) is included as a reference.*

Table 1: *Model name and implemented measurements used in the radiative transfer simulations.*

Model name	Parameters	Short name
afglsw	standard atmosphere	A
Dropsonde	A + pressure form dropsonde	B
Dropsonde + humidity	B + humidity of CR-2	C

like water vapour. Table 1 lists the three different models and corresponding parameters. The vertical resolution of the model was increased to 50 m steps between 0 m and 500 m and to 100 m between 500 m and 1 000 m. Above 1 000 m the difference between the model layers is set to 200 m. Concentrations of ozone, oxygen, carbon dioxide and nitrogen dioxide are adapted from the standard atmosphere profile and interpolated to the hight levels considering the model temperature and pressure profile. The composition of gases in the atmosphere do not change significantly which justifies linear interpolation. For surface temperature a value of 260.50 K was set corresponding to $-12.56\,^{\circ}$C which was measured by a ground based station at Inuvik.

For temperature retrieval the calculations were started and resulting simulation were compared with the measured profiles of upward / downward brightness temperature for the first hight level. Changing the temperature in the model atmosphere the modelled brightness temperature was fitted to the converted brightness temperature from the irradiance measurement. This process was repeated until best agreement between simulation and measurement for all hight levels was achieved. This was performed for upward and downward brightness temperature separately. In Fig. 4 a) measured upward brightness temperature is plotted (solid line). The grey highlighted area marks the uncertainty range of the pyrgeometer with $\pm 1.2\,$K. The other lines show simulated profiles of brightness temperature resulting from the adapted modelling temperature profile. The model temperature was changed beginning at the bottom and going upward. In Fig. 4 b) the dif-

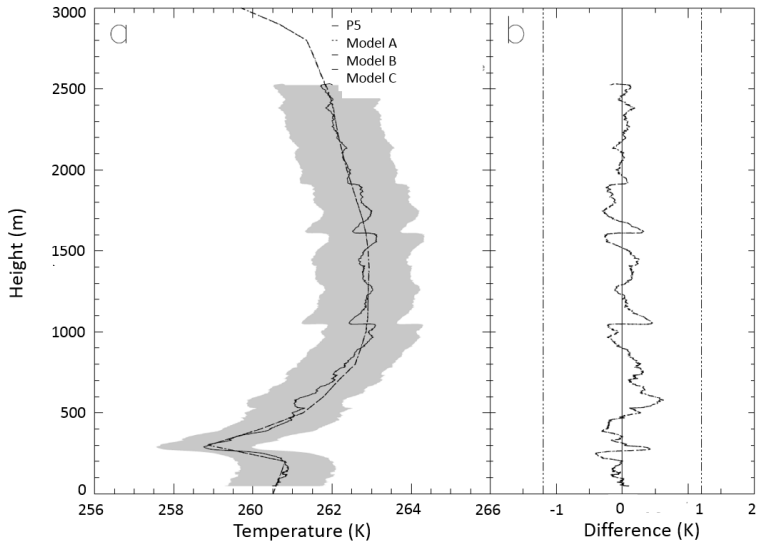

Figure 4: *Left: Measured vertical profile of brightness temperature (solid line) using the upward irradiance. The uncertainty range of the CGR4 is indicated by the grey area. Resulting modelled profiles of brightness temperature by the models are indicated by the dashed and dotted lines. Right: Differences of measured and modelled brightness temperature.*

ferences between measured and modelled brightness temperature are plotted. All three simulations are fitted close to the measurement. The differences are always within the uncertainty range. Only between 250 m and 300 m a spike of 1.7 K exceeds the uncertainty range. This is caused by an inversion and the resulting gradient which could not be represented in the model completely. Between 400 m and 1 000 m the differences are small. Below 1 000 m the simulations systematically overestimate the measurement. Contrarily, above 1 000 m the measurement is underestimated by the models. Similar to Fig. 4, Fig. 5 shows the vertical brightness temperature profile calculated from the downward irradiance measurements. The adaption of the model temperature profile started at 3 000 m going to the bottom. Much larger differences between model and measurement are obvious compared to Fig. 4. Model A and B agree well with the measurement and are mostly inside of the uncertainty range of the pyrgeometer. The plot of model B is fitting slightly better indicating the importance of utilizing pressure measurements in the simulations. In contrast, model C completely disagrees with the other models and the measurement. Additionally applying humidity measurements in model C instead of assumptions the results should agree best which is not the case. One possible reason are the different profiles of relative humidity measured by CR-2 and the dropsonde. As shown in Fig. 2 the humidity profile of the CR-2 is lower compared to the dropsonde measurement. Nevertheless, model C follows the general pattern with a negative offset which has to be considered with respect to low relative humidity. This indicates that for retrievals utilizing downward irradiance precise measurements of pressure and humidity are needed. Furthermore, measured profiles of humidity and pressure above the retrieval hight have to be available. This is most important for retrievals using the downward irradiance because upper laying atmospheric layers influence the radiation profile of the atmosphere below. Using the downward irradiance the temperature retrieval shows significant disagreement between model and measurement. For all heights a systematically

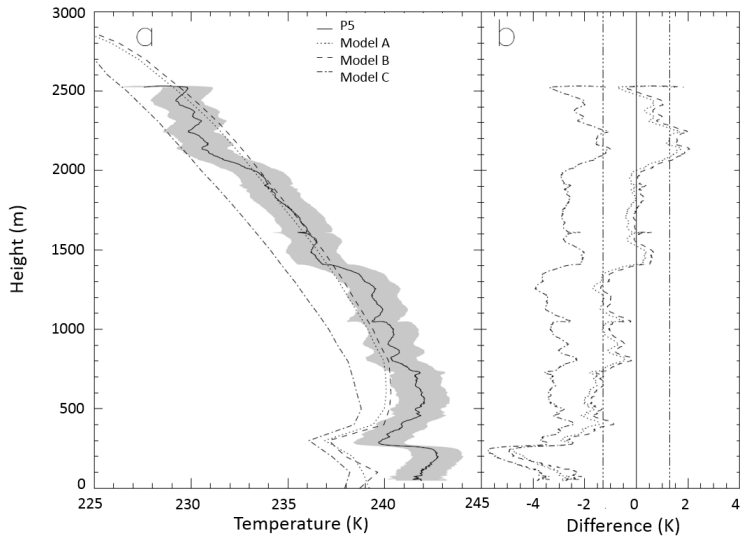

Figure 5: *Left: Measured vertical profile of brightness temperature (solid line) using the downward irradiance. The uncertainty range of the CGR4 is indicated by the grey area. Resulting modelled profiles of brightness temperature by the models are indicated by the dashed and dotted lines. Right: Differences of measured and modelled brightness temperature.*

underestimation of the temperature profile is present. This indicates that measurements of upward irradiance are suited better for retrieval of vertical temperature profiles from irradiance measurements. Therefore the following retrieved temperature profile was obtained from upward irradiance measurements.

Fig. 6 a) shows the measurement of the P5 sensor (solid line) and the retrieved vertical temperature profiles of the three different models (dashed lines). Fig. 6 b) shows the deviation between modelled and measured temperature. The uncertainty range of $\pm 0.25\,^{\circ}\mathrm{C}$ of the P5 sensor is highlighted by the grey area in a) and the dash-dotted vertical lines in b). All three model profiles show the same pattern. The largest discrepancy appears between 0 m and 500 m because of the strong gradient in irradiance resulting from the inversion layer and corresponding stratiform clouds. This could not be represented in the model simulations because of low hight resolution. Between 500 m and 1 100 m the modelled profiles are within the uncertainty range of the P5 sensor and therefore in good agreement. Above 1 100 m all three models overestimate the measured temperature with increasing difference with hight but not exceeding 2 K.

It is assumed that the strong differences between modelled and measured temperature profile around 300 m are due to clouds which influence the radiative transfer significantly and have to be considered in the model. This shows that the temperature does not determine the profile of terrestrial radiation alone. In addition the humidity profile has to be considered as realized in this case by CR-2 and dropsonde measurement. Another possible reason is condensation on the pyrgeometer domes resulting from flying in suddenly changing air masses. Climbing out of cool and dry air into a more humid and warmer airmass water droplets may condensate on the pyrgeometer dome causing a sudden increase of irradiance and resulting higher brightness temperature. Also spatial differences between the different measured profiles have to be considered. In the presented case the ascent from 50 m to 2 500 m took 14 minutes. The aircraft flew with

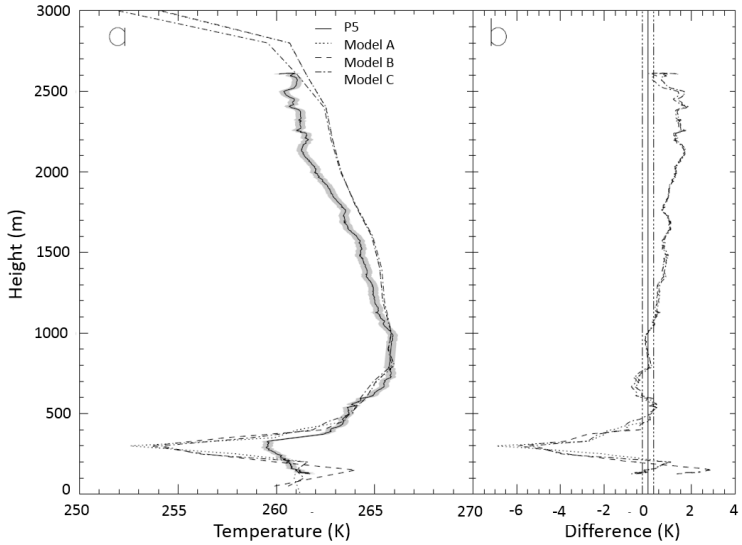

Figure 6: *Left: Profile of vertical temperature measured by P5 (solid line) and corresponding uncertainty range (grey). The retrieved temperature profiles of the models are indicated by the dashed and dotted lines. Right: Difference between measured and modelled temperature profiles.*

55 $\mathrm{m\,s^{-1}}$ and covered a distance of 48 km. Therefore environmental conditions like surface albedo, surface temperature and humidity change which also influence the upward and downward radiative profiles.

5 Conclusion

A retrieval of vertical temperature profiles from measured upward and downward irradiances in the infrared wavelength region was performed. The radiative transfer simulations include the meteorological parameters humidity and pressure measured during the flight. These measurements have to be supported by ground-based data from observation sites and nearby radiosonde launches. Comparison of derived temperature profiles from upward and downward irradiance revealed that the upward profile leads to better results because it is not influenced by the overlying atmospheric layers. Downward irradiance can be influenced by clouds and supersaturated atmospheric layers and causes bias in the temperature retrieval. Therefore, humid layers have to be implemented in the model simulations to avoid temperature profiles with strong gradients as happened in the presented case. Additionally the surface temperature has to be considered when using upward irradiance because this influences the vertical temperature profile. Therefore ground-based measurements of the surface temperature are crucial and must be implemented in the models. First simulations using upward irradiance show good agreement between model output and measured temperature profile being inside the measurement uncertainty. Furthermore stable atmospheric conditions are preferred and situations with inversions should avoided.
To improve this retrieval technique further investigation is necessary. Applying an advanced iterative algorithm which changes the input temperature of the model automatically will accelerate the retrieval process. An increase of the vertical resolution of the radiative transfer model from 50 m to 10 m is suggested to obtain temperature profiles

with higher resolution. This also reduces deviations between retrieved and measured temperature profile resulting from gradients in the radiation profile.

References

Anderson, G., Clough, S., Kneizys, F., Chetwynd, J., and Shettle, E.: AFGL Atmospheric Constituent Profiles (0–120 km), Tech. Rep. AFGL-TR-86-0110, AFGL (OPI), Hanscom AFB, MA 01736, 1986.

Buck Research Instruments, L.: Model CR-2 Hygrometeor Operating Manual, Boulder, 2009.

Geiger, R., Aron, R. H., and Todhunter, P.: The climate near the ground, Vieweg, 1995.

Kempler, S.: AIRS Atmospheric InfraRed Sounder, URL `disc.gsfc.nasa.gov/AIRS`, 2013.

Kipp & Zonen: CGR4 Pyrgeometer Operations Manual, Delft, 2006.

Mayer, B. and Kylling, A.: Technical note: The *libRadtran* software package for radiative transfer calculations - description and examples of use, Atmos. Chem. Phys., 5, 1855–1877, 2005.

Petty, G.: A First Course in Atmospheric Radiation, 2nd Edition, Sundog Publishing, Madison, Wisconsin, 2006.

Pithan, F. and Mauritsen, T.: Arctic amplification dominated by temperature feedbacks in contemporary climate models, Nature, 7, 181–184, doi:10.1038/ngeo2071, 2014.

Pospichal, B.: Bodengebundene Messgeräte zur Fernerkundung der Atmosphäre am Leibniz-Institut für Troposphärenforschung (IfT) in Leipzig, 2011.

Stickney, T. M., Shedlov, M. W., and Thompson, D. I.: Goodrich Total Temperature Sensors Technical Report 5755, Rosemount Aerospace Inc., 1994.

Vaisala: Vaisala Dropsonde RD94 Manual, 2010.

Wendisch, M. and Yang, P.: Theory of Atmospheric Radiative Transfer - A Comprehensive Introduction, Wiley-VCH Verlag GmbH & Co. KGaA, Weinheim, Germany, iSBN: 978-3-527-40836-8, 2012.